ACEEE Int. J. on Signal & Image Processing, Vol. 4, No. 1, Jan 2013

Lung Nodule Segmentation in CT Images using Rotation Invariant Local Binary Pattern

G. Deep[1] L. Kaur[2], and S. Gupta[3]
[1]Chandigarh Engg. College (CEC)/Department of CSE, Landran-140307, Mohali, India
E-mail: gaganpec@yahoo.com
[2] Punjabi University/Department of CE, UcoE, Patiala, India
[3]Panjab University/Department of CSE, UIET, Chandigarh, India
E-mail: {mahal2k8, savita2k8}@yahoo.com

***Abstract*—As the lung cancer is the leading cause of cancer death in the medical field, Computed Tomography (CT) scan of the thorax is widely applied in diagnoses for identifying the lung cancer. In this paper, a technique of rotation invariant with Local Binary Pattern (LBP) for segmentation of various lung nodules from the Lung CT cancer data sets is used. This is tested on various lung data sets from teaching files of Casimage database and National Cancer Institute (NCI) of National Biomedical Imaging Archive (NBIA). The results show the segmented nodules with clear boundaries, which is helpful in diagnosis of lung cancer. Further, the results are compared with the watershed segmentation method, which shows that LBP based method yields better segmentation accuracy.**

***Index Terms*—Image Segmentation, Lung Nodules, CT, LBP, MATITK.**

I. Introduction

Cancer is the second most common cause of death in the United States after heart disease, accounting for 1 in every 4 deaths [1]. As reported by American Cancer Society on cancer, about 1.6 million Americans were diagnosed with cancer in 2011 and 571,950 died of cancer, more than 1,500 people a day. In the past two decades numerous screening studies have been conducted worldwide to study early indications of lung cancer. Indeed, survival of lung cancer is strongly dependent on accurate and early diagnosis [2]. For identifying the lung nodules, Computed Tomography (CT) scan of the thorax is widely applied in diagnosis. The rapid developments in chest CT acquisition techniques have been followed by a sharp increase in research on computer analysis of thoracic CT scans. Compared to other modalities, CT excels in the imaging of the lungs [3]. The preprocessing step of most Computer-Aided Diagnosis (CAD) systems for identifying the lung diseases is lung segmentation [4] [5]. The purpose of the segmentation is to separate human body regions from background and make an initial classification showing the right and left lung clearly. For the detection of any lung disease, it is further segmented to extract the exact ROI like lung nodules in the case of cancer detection [6] [7]. Hu et al. [8] described a method of global thresholding for the segmentation. Pohle and Toennies [9] suggested adaptive region growing method for segmentation of medical images. Most of segmentation methods are based on morphological operations [10]. But the results are not satisfied as judged by physicians. Various automatic tools like Analyze 10.0 [12], Mazda [13], YaDiv [14] on CT are also suggested. Vincent Chu et al. [15] proposed MATLAB based tool called MATITK that uses the watershed algorithm for segmentation. This has given good results in lung segmentation especially for high volume dataset [11]. There is no loss of lung nodules but problem was the clear visualization. However, many papers are published on plain rotation invariance analysis [21,22,23]. A number of techniques incorporating invariance with respect to both spatial scale and rotation have been developed [24, 25]. For the segmentation of Lung nodules on CT images, Rotation invariant Local Binary Pattern (LBP) [16] has shown very effective results. This helps in clear visualization of nodule boundaries which is important for doctors for analyzing the disease effects.

II. Segmentation In Medical Imaging

Segmentation has an important role in medical imaging as it helps in extracting the organ of interest. For the diagnosis of lungs, it is necessary to segment the chest images and extract the lungs in the preprocessing step and further the nodules are segmented with the different methods. One pulmonary CT image as shown in figure 1 is a precursor to most pulmonary image analysis applications.

Figure 1.The lung Cancer Image in which lung parenchymas seen as the dark region in the body. The surrounding tissue appears with a higher intensity

A. Preprocessing Step: Lung Segmentation (to Separate Lung Parenchymas)

By using the following steps, firstly lung area is separated from background [17] of the lung CT images as shown in

DOI: 01.IJSIP.4.1.9

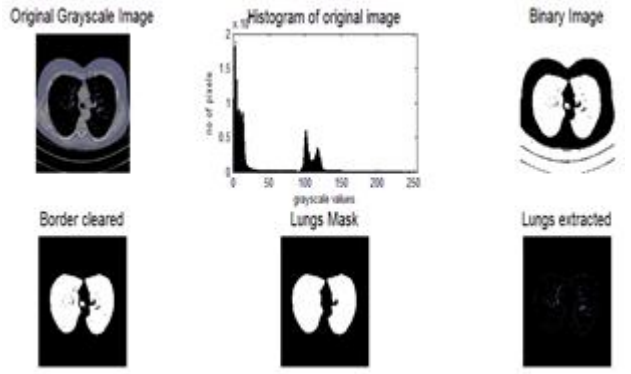

Figure 2. Separation of Lungs after the removal of mediastinum (a) Original DICOM CT Lung Image from LIDC (b) Thresholding point using histogram (c) Binary Image (d) Cleaning (e) Lung Mask (f) Lungs Extraction

figure 2.

1. Optimal Thresholding: The image is thresholded to separate low-density tissue (eg. Lung parenchymas) from fat.
2. Background removal: The surrounding air, identified as low–density tissue, is removed.
3. Cleaning: It is performed to fill the holes in the binary image.
4. Lung mask: To extract lungs from background, lung mask is created.
5. Lung Extraction: Output of step 4 is subtracted from the original image to provide separated lungs for further processing.

B. Rotation Invariant Local Binary Pattern (LBP) for lung nodule Segmentation

Local Binary Pattern (LBP) [16]: After finding out the lungs parenchymas from the preprocessing step, rotation invariant and gray scale invariance using Local Binary Operator is applied to get the lung nodules. The local binary pattern operator is theoretically simple, yet very powerful and gray-scale invariant method of analyzing textures [18] to do the segmentation. In practice, the LBP operator combines characteristics of statistical and structural texture analysis: it describes the texture with micro-primitives, often called textons, and their statistical placement rules [19]. Another important property is its computational simplicity, which makes it possible to analyze images in challenging real-time settings.

Starting from the joint distribution of gray values of a circularly symmetric neighbor set of eight pixels in a 3x3 neighborhood, there is an operator that is by definition invariant against any monotonic transformation of the gray scale. The dimensionality of the *LBP* feature distribution can be calculated according to the number of neighbors used. The definition of the *LBP* has been extended to arbitrary circular neighborhoods of the pixel to achieve multi-scale analysis and rotation invariance [16,20]. Rotation invariance is achieved by recognizing that gray scale invariant operator incorporates a fixed set of rotation invariant patterns.

The value of the *LBP* code of a pixel (x_c, y_c) is given by:

$$LBP_{P,R} = \sum_{p=0}^{P-1} s(g_p - g_c)2^p, s(x) = \begin{cases} 1, & if\ x \geq 0; \\ 0, & otherwise; \end{cases} \quad (1)$$

Where

g_c: gray value of the center pixel

g_p: gray values of the circularly symmetric neighborhood $g_p\ (p = 0, \ldots, p\text{-}1)$.

P: Image Pixels in the circle of radius $R(R > 0)$ that form a circularly symmetric neighbor set

2^p: binomial factor for each sign $s(g_p - g_c)$

Since the LBP is invariant to monotonic changes in gray scale, it is supplemented by an orthogonal measure of local contrast. Below example shows how the contrast measure (C) is derived. The average of the gray levels below the center pixel is subtracted from that of the gray levels above (or equal to) the center pixel. Two-dimensional distributions of the LBP and local contrast measures are used as features. The operator is called *LBP/C*.

An example of computing *LBP* and Contrast measure (*C)* in a 3*3 neighborhoods:

example			thresholded			weights		
6	5	2	1	0	0	1	2	4
7	6	1	1		0	128		8
9	8	7	1	1	1	64	32	16

Pattern = 11110001

LBP = 1 + 16 + 32 + 64 + 128 = 241

C = (6+7+8+9+7)/5 – (5+2+1)/3 = 4.7

Important properties are:

- *LBP* is invariant to any monotonic grey level change
- Computational simplicity

To remove the effect of rotation, i.e. to assign a unique identifier to each rotation invariant local binary pattern, rotation invariance is defined, formally:

$$LBP_{P,R}^{ri} = min\left\{\mathrm{ROR}(\mathrm{LBP}_{P,R}, i) \middle| i = 0, \ldots, P-1\right\} \quad (2)$$

Where *ROR(x,i) function* performs a circular bit-wise right shift on the P-bit number *x*,i times.

To quantify the varying performance of individual patterns attributes to the spatial structure of the patterns, a uniformity measure U ('pattern') is defined, which corresponds to the number of spatial transitions (bitwise 0/1 changes) in the 'pattern'. These patterns are called "uniform" because they have one thing in common: at most two one-to-zero or zero-to-one transitions in the circular binary code. However, only limited subsets of 'uniform' patterns are used instead of all rotation invariant patterns, which improve the rotation invariance considerably. So, this operator is called as $LBP_{8,R}^{riu2}$. The use of 'uniform' patterns only is motivated by the reasoning that they tolerate rotation better because they contain fewer spatial transitions exposed to unwanted changes upon rotation.

The *LBP* operator is an excellent measure of the spatial structure of local image texture, but it discards the other important property of local image texture, contrast, since it de-

DOI: 01.IJSIP.4.1.9

pends on the gray scale. If only rotation invariant texture analysis is desired, i.e., gray-scale invariance is not required. The performance of *LBP* is further enhanced by combining it with a rotation invariant variance measure *VAR* that characterizes the contrast of local image texture.

$$VAR_{P,R} = \frac{1}{P}\sum_{p=0}^{P-1}(g_p - \mu)^2 \ ,where\ \mu = \frac{1}{P}\sum_{p=0}^{P-1} g_p \quad (3)$$

VAR_8 is invariant against shifts in gray scale. Since *LBP* and *VAR* are complementary, the joint distributions LBP_8^{riu2}/VAR_8 (aka *LBPV*) is very powerful rotation invariant measure of local image texture [16]. The combined operator *LBPV* separates the textures providing clear boundaries resulting in very efficient segmentation of image.

III. Experimental Results

In this study, the performance of rotation invariant LBP algorithm and watershed algorithm is analyzed on Lung Image Database Consortium (LIDC) public lung image database. The LIDC data have been collected from five different sites in the United States [28]. Watershed algorithm for volumetric segmentation using MATLAB Insight Segmentation and Registration Toolkit (MATITK) has used for lung segmentation [15, 17]. But still MATITK is under observation by some researchers as it is highly dependent upon the dataset. MATITK can be used only on 3D images, but Fig 3, shows the result of watershed segmentation on one slice of an image. There is no mechanism available to see all the 3d slices in MATITK. Using View3D[1] function, the segmentation of all the slices can be seen.

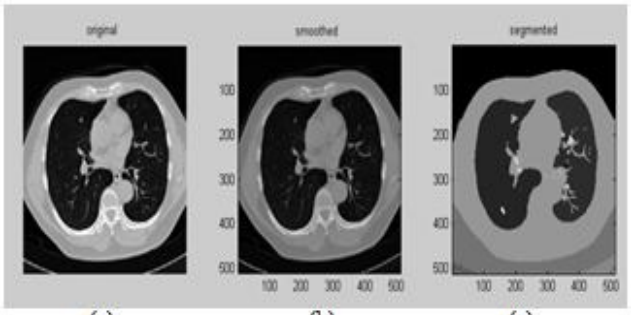

Figure 3. (a) Original Lung CT Image (b) Filtered Image (c) Segmented Image by Watershed Algorithm

On the other hand, the rotation invariant *LBP* uniform pattern image $LBP_{1,8}^{ri}$ and correspondingly histogram of the lung segmented nodules showing texture variance features after finding out the uniform pattern in figure 4(a) and 4(b) respectively. The final combined operator *LBPV* separates the textures with clear boundaries resulting in very efficient segmentation of image as shown in figure 5.

Using SIENET Sky Dicom viewer tool [26] and RadiAnt DICOM viewer tool [27], segmentation of all the slices of medical images can be viewed efficiently. In the Table 1, the average accuracy[2] of the segmentation by the rotation invariant LBP Variance Operator is 98% over the accuracy of 86% by MATITK method applied on 3 patient data sets of LIDC database [28].

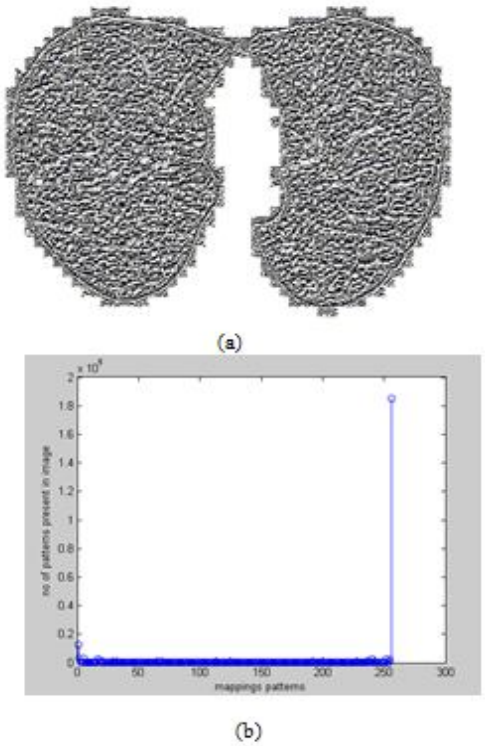

Figure 4. (a) Rotation Invariant LBP Uniform Pattern Image LBP^{riu}
(b) Histogram showing LBP Image using rotation invariant pattern of Image

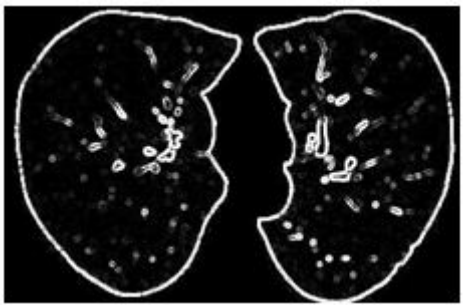

Figure 5. Segmentation of Lung Nodules using Combined LBPV operator

Table I. Segmentation Average Accuracy

Patient ID	Image number	Segmentation Accuracy by Watershed Algorithm	Segmentation Accuracy by LBP
1.3.6.1.4.1.93 28.50.3.0047	00060.jpg	86.0712	98.5101
	00061.jpg	86.0003	98.5650
1.3.6.1.4.1.93 28.50.3.0050	00059.jpg	85.7899	98.4600
	00060.jpg	85.7199	98.5101
1.3.6.1.4.1.93 28.50.3.0041	00135.jpg	85.7003	98.5891
	00136.jpg	85.6993	98.6049

IV. Conclusion and Future Scope

Though automatic segmentation is desirable but manual intervention in medical diagnosis is indispensable therefore,

[1] view3d.sourceforge.net/

DOI: 01.IJSIP.4.1.9

Local Binary operator is used for gray-scale and rotation invariant texture classification. The approach is based on uniform patterns and nonparametric discrimination of sample and prototype distributions. Uniform patterns help to recognize texture microstructures such as edges. The operator performs well for the structural and stochastic patterns. Further, to show the efficacy of LBP based method, the results are compared with the watershed algorithm. The comparison indicates that LBP is very effective in segmenting the lung nodules on CT images and also gives the improved average segmentation accuracy over the watershed method which is further helpful in diagnosis of lung cancer.

Segmented nodules can be further matched with different types of lung nodule templates for the retrieval of abnormal nodule, so that early retrieval of cancer can be done.

REFERENCES

[1] American Cancer Society. Factbox: Latest U.S. cancer statistics, American Cancer Society, Atlanta, GA, 2011. http://www.reuters.com/article/2011/06/17/us-factbox-cancer-idUSTRE75G0PL20110617

[2] United states national institute of health. www.nih.gov.

[3] M. Prokop I. Sluimer, A. Schilham and B. van Ginneken, "Computer analysis of computed tomography scans of the lung: A survey", IEEE Transactions on Medical Imaging, vol. 25(4), pp. 385-405, 2006.

[4] P. Singh, S. Singh, G. Kaur, "A study of gaps in CBMIR using different methods and prospective", Proceedings of world academy of science, engineering and technology, vol. 36, pp. 492-496, 2008.

[5] Zhen Ma, João Manuel R. S. Tavares, R. M. Natal Jorge, "A review on the current segmentation algorithms for medical images", 1st International Conference on Imaging Theory and Applications (IMAGAPP), INSTICC Press, pp. 135-140, 2009.

[6] Holli et al.,"Texture analysis of MR images of patients with mild traumatic brain injury", BMC Medical Imaging, vol. 10(8), 2010.

[7] Alexander S. Behnaz, James Snider, Chibuzor Eneh, "Quantitative CT for volumetric analysis of medical images: initial results for liver tumors", Medical Imaging 2010, Proc. of SPIE, vol. 7623-76233U, 2010.

[8] S. Hu, E. A. Ho_man and J. M. Reinhardt, "Automatic lung segmentation for accurate quantitation of volumetric x-ray CT images", In IEEE Transactions on Medical Imaging, vol. 20(6), 2001.

[9] Regina Pohle and Klause D. Toennies, "Segmentation of medical Images using adaptive region growing", Department of Simulation and Graphics, Proc. SPIE Medical Imaging, pp.1337-1346, 2001.

[10] Hye Suk Kim , Hyo-sun Yoon , Kien Nguyen Trung, and Guee Sang Lee, "Automatic lung segmentation in CT images using anisotropic diffusion and morphology operation", Seventh International Conference on Computer and Information Technology, IEEE Computer Society, pp. 557-561, 2001.

[11] Rushin Shojaii , Javad Alirezaie, Paul Babyn, "Automatic lung segmentation in CT images using watershed transform", IEEE conference, vol.2, pp. 1270-1273, 2005.

[12] Richard A. Robb, "The biomedical imaging resource at mayo clinic- guest editorial", IEEE Transactions on Medical Imaging, vol. 20(9), pp. 854-867, 2001.

[13] Piotr M. Szczypiński, Micha³ Strzelecki, Andrzej Materka, Artur Klepaczko, "MaZda-A software package for image texture analysis", Elsevier, Computer Methods and Programs in Biomedicine, vol. 94(1), pp. 66-76, 2009.

[14] K, K., & M, S., "Patient-oriented segmentation and visualization of medical data", Proceedings of CGIM, University of Maryland, Human Computer Interaction Lab, pp. 214-219, 2002.

[15] Vincent Chu and Ghassan Hamarneh, "MATLAB-ITK interface for medical image filtering, segmentation and registration", Medical Imaging 2006: Image Processing, Proc. of SPIE, vol. 6144, 61443T1-8, 2006.

[16] Ojala, T., Pietikäinen, M., Mäenpää, T., "Multiresolution gray-scale and rotation invariant texture classification with local binary patterns", IEEE Transaction, vol.24, pp. 971–987, 2002.

[17] Heuberger, J., Geissbuhler, A., Muller, H., "Lung CT segmentation for image retrieval using the insight toolkit (ITK)". Medical Imaging and Telemedicine, (MIT2005), Hopitaux University of Geneva, China, 2005.

[18] Ojala, T., PietikaÈinen, M., Harwood, D., "A comparative study of texture measures with classification based on feature distributions", Pattern Recognition, vol. 29, pp. 51-59, 1996.

[19] Haralick, R.M., "Statistical and structural approaches to texture", Proc IEEE 67, vol.5, pp-786-804, 1979.

[20] Pietikainen, M., Ojala, T., Xu, Z., "Rotation-Invariant texture classification using feature distributions", Pattern Recognition, vol.33, pp. 975-985, 2000.

[21] Lam, W.-K., Li, C.-K., "Rotated texture classification by improved iterative morphological decomposition". IEE Proc - Vision, Image and Signal Processing, vol.144, pp.171-179, 1997.

[22] Madiraju, S.V.R., Liu, C.C., "Rotation invariant texture classification using covariance". Proc. Int. Conf. Image Processing, pp. 262-265. Washington, D.C., 1995.

[23] Mao, J., Jain, A.K., "Texture classification and segmentation using multiresolution simultaneous autoregressive models", vol. 25, pp.173-188, 1992.

[24] Manian, V., and Vasquez, R., "Scaled and rotated texture classification using a class of basis functions", Pattern Recognition, vol. 31, pp. 1937-948, 1998.

[25] Wu, Y., and Yoshida, Y., "An efficient method for rotation and scaling invariant texture classification", Proc. IEEE Int'l Conf Acoustics, Speech, and Signal Processing, vol.4, pp. 2519-2522, 1995.

[26] Siemens Corporation, "SIENET Sky – DICOM CD Viewer" http://www.webbuyersguide.com/Product/viewproduct.aspx?id=42372

[27] Maciej Frankiewicz, "http://www.radiantviewer.com/", Poland.

[28] Kascic, E., NBIA - National Cancer Imaging Archive NCIA (version 4.0): The NCI's repository for DICOM-based images (https://cabig.nci.nih.gov/tools/NCIA)

[2]en.wikipedia.org/wiki/Accuracy_and_precision

DOI: 01.IJSIP.4.1.9